

RVC OPEN ACCESS REPOSITORY – COPYRIGHT NOTICE

This is the peer reviewed version of an accepted journal article:

Booler, H. S., Williams, J. L., Hopkinson, M. and Brown, S. C. (2015), Degree of Cajal–Retzius Cell Mislocalization Correlates with the Severity of Structural Brain Defects in Mouse Models of Dystroglycanopathy. *Brain Pathology*. doi: 10.1111/bpa.12306

which has been published in final form at <http://dx.doi.org/10.1111/bpa.12306>. This article may be used for non-commercial purposes in accordance with [Wiley Terms and Conditions for Self-Archiving](#)."

The full details of the published version of the article are as follows:

TITLE: Degree of Cajal-Retzius cell mislocalisation correlates with the severity of structural brain defects in mouse models of dystroglycanopathy

AUTHORS: Helen S. Booler, Josie L. Williams, Mark Hopkinson and Susan C. Brown

JOURNAL TITLE: *Brain Pathology*

VOLUME/EDITION:

PUBLISHER: Wiley

PUBLICATION DATE: 12 October 2015

DOI: 10.1111/bpa.12306

1
2
3
4 Degree of Cajal-Retzius cell
5
6 mislocalisation correlates with the
7
8 severity of structural brain defects in
9
10 mouse models of dystroglycanopathy.
11
12
13
14
15

16 Helen S. Booler, Josie L. Williams, Mark Hopkinson, Susan C. Brown.
17
18
19

20
21 Department of Comparative Biomedical Sciences, Royal Veterinary College, London NW1 0TU.
22
23
24

25 Author for correspondence:- Dr. Susan C. Brown
26
27

28 Email: scbrown@rvc.ac.uk.
29

30 Telephone: +44 20 74681212
31
32
33

34 Key Words: dystroglycan, neuronal migration, reelin, Cajal-Retzius cells, Pial Basement membrane,
35
36 congenital muscular dystrophy.
37

38 Running title: Brain defects in the dystroglycanopathies
39
40
41
42
43
44
45
46
47
48
49
50
51
52
53
54
55
56
57
58
59
60

Abstract

The secondary dystroglycanopathies are characterised by the hypoglycosylation of alpha dystroglycan, and are associated with mutations in at least 18 genes which act on the glycosylation of this cell surface receptor rather than the *Dag1* gene itself. At the severe end of the disease spectrum, there are substantial structural brain defects, the most striking of which is often cobblestone lissencephaly. The aim of this study was to determine the gene-specific aspects of the dystroglycanopathy brain phenotype through a detailed investigation of the structural brain defects present at birth in three mouse models of dystroglycanopathy - the FKR^{KD} which has an 80% reduction in *Fkrp* transcript levels; the *Pomgnt1*_{null}, which carries a deletion of exons 7-16 of the *Pomgnt1* gene; and the *Large*^{myd} mouse, which carries a deletion of exons 5-7 of the *Large* gene. We show a rostrocaudal and mediolateral gradient in the severity of brain lesions in FKR^{KD}, and to a lesser extent *Pomgnt1*_{null} mice. Furthermore, the mislocalisation of Cajal-Retzius cells is correlated with the gradient of these lesions and the severity of the brain phenotype in these models. Overall these observations implicate gene specific differences in the pathogenesis of brain lesions in this group of disorders.

Introduction

The dystroglycanopathies are a heterogeneous group of neuromuscular diseases, associated with mutations in genes that encode proteins implicated in the glycosylation of alpha dystroglycan rather than the *Dag1* gene itself. As a consequence these are referred to as 'secondary' rather than primary. Rare mutations in the *Dag1* gene have been reported but they amount to only a few cases due most likely to embryonic lethality (27). To date, mutations in at least 18 genes have been associated with the secondary dystroglycanopathies, many of which encode either proven or putative glycosyl transferases. These include POMGNT1, which is a demonstrated glycosyltransferase adding N-acetylglucosamine (88); LARGE, a bifunctional glycosyltransferase that alternately transfers xylose and glucuronic acid and confers ligand binding (25, 38, 50, 79), and Fukutin-related protein (FKRP), the function of which is currently unknown (7, 10, 12). Interestingly, mutations in these genes are associated with a wide spectrum of clinical phenotypes, which at the severe end of the disease spectrum include congenital muscular dystrophies with structural brain defects, exemplified by Walker Warburg syndrome (WWS) OMIM 236670, Muscle Eye Brain disease (MEB) OMIM 253280, congenital muscular dystrophy type 1 C (MDC1C) OMIM 606612 and congenital muscular dystrophy type 1D (MDC1D) OMIM 608840. Severely affected patients typically show a range of structural brain abnormalities associated with defects in neuronal migration, particularly type II (cobblestone) lissencephaly, which is strongly suggestive of this group of disorders (17). In addition, patients may show cortical and cerebellar dysplasia, polymicrogyria and hydrocephalus, with evidence of dysmyelination on MRI (9). Work in dystroglycanopathy patients and mouse models, strongly suggests that the hypoglycosylation of alpha dystroglycan is central to the pathogenesis via its effect on the structural integrity of the pial basement membrane during cortical development (56, 59).

Dystroglycan (DG) is transcribed from a single gene (*Dag1*) and undergoes post-translational cleavage to produce the peripheral membrane protein alpha dystroglycan, and the transmembrane protein beta dystroglycan, which are non-covalently linked (37). Alpha dystroglycan undergoes extensive O-linked mannosylation of its central mucin-rich domain, and these glycan chains mediate binding to extracellular matrix proteins such as laminin (20), agrin (23, 86), neuexin (74), pikachurin (69) and perlecan (57). Beta dystroglycan in

turn interacts with the cell's actin cytoskeleton via dystrophin, utrophin, ezrin or plectin (57). Together, alpha and beta dystroglycan effectively link the cytoskeleton to the extracellular matrix. The DG complex has been previously demonstrated to play a primary role in the deposition, organisation and turnover of basement membranes (31).

Targeted deletion of dystroglycan in the brain during development, or mutations of known or putative glycosyltransferases involved in the glycosylation of alpha dystroglycan, have both been demonstrated previously to recapitulate many aspects of WWS and MEB, indicating dystroglycan as central to the disease pathogenesis (1, 25, 49, 58). However, in the absence of comparative studies it is unclear whether some aspects of the neuropathologic lesions are gene specific. In order to answer this question, we have now undertaken a detailed investigation of the structural brain defects in three dystroglycanopathy mouse models – the FKRP-Neo^{Tyr307Asn} (FKRP^{KD}) which has an 80% reduction in *Fkrp* transcript levels (1); the Pomgnt1_{null} mouse, which carries a deletion of exons 7-16 of the *Pomgnt1* gene; and the Large^{myd} mouse, which carries a deletion of exons 5-7 of the *Large* gene (25).

Materials and Methods

Mouse models and Genotyping.

Three dystroglycanopathy mouse models were compared – the FKRP-Neo^{Tyr307Asn} (FKRP^{KD}) (1); the Pomgnt1_{null}, and the Large^{myd} (25). The POMGnT1_{null} strain used for this piece of work was generated by the Functional Glycomic Consortium (Pomgnt1^{tm1.1Cfgr}/Mmucd) and has a deletion of exons 7-16 of the *Pomgnt1* gene. All animal experiments were carried out under license from the Home Office (UK) in accordance with The Animals (Scientific Procedures) Act 1986 and were approved by the Royal Veterinary College ethical committee. Mice were sacrificed at P0 and genotype was confirmed by PCR. Primers were as follows: for FKRP^{KD} mice, *Fkrp* forward: GTTGTGCTTAAACCACCTTC; *Fkrp* neo forward: GGTGGGATTAGATAAATGCC; *Fkrp* reverse: CTAGGAGGTTGAGGATGATGG. *Fkrp* forward and *Fkrp* reverse amplified the wild type gene, *Fkrp* neo forward and *Fkrp* reverse the mutant gene. For Pomgnt1_{null} mice, primer 1607: CTGGGCCACACAAGTCATGA; primer 1608: TCTCTGCTCAAACGCTGCCC; primer 1796: TTGATGCTGTTATAGAGGCC. Primers 1607 and 1608 amplified the wild type gene, primers 1607 and 1796 the mutant gene. For the Large^{myd}, primers were MydF3: ATCTCAGCTCCAAAGGGTGAAG; MydR2:

1
2
3 GCCAATGTAAAATGAGGGGAAA; GT4F: GGCCGTGTTCCATAAGTTCAA; GT4R:
4 GGCATACGCCTCTGTGAAAAC. MydF3 and MydR2 primers amplified the mutant gene and
5
6 GT4F and GT4R the wild type.
7

8 Histology

9
10 The heads were fixed in Bouin's fixative (Sigma) for 24 hours at room temperature, before
11 being processed and embedded in paraffin wax. Samples were serially sectioned at 5µm,
12 with sections collected onto charged slides (Superfrost Plus, VWR). At approximately 50µm
13 intervals, sections were stained with haematoxylin and eosin (HE). Intermediate levels were
14 retained for immunohistochemistry.
15
16
17
18

19 Immunohistochemistry

20
21 Primary antibodies used in the study were as follows: rabbit anti-brain lipid binding protein
22 1:300 (raised against human brain lipid binding protein, rabbit polyclonal, ABN14, Millipore),
23 mouse anti-reelin 1:1000 (raised against recombinant fusion protein, corresponding to
24 amino acids 164-496 of mouse reelin, monoclonal clone name G10 Abcam), and anti- alpha
25 dystroglycan (IIH6)1:200 (raised against rabbit skeletal muscle membrane preparation,
26 monoclonal, clone name IIH6C4, Millipore). Sections were deparaffinised and rehydrated.
27 Heat-induced epitope retrieval (HIER) was performed in Tris-EDTA (10 mM Tris-HCl, 1 mM
28 disodium EDTA, pH 8.0). All primary antibodies were diluted in phosphate buffered saline
29 containing 0.05% tween 20 (Sigma) and 5% goat serum (Sigma), and sections were
30 incubated for 1 hour at room temperature. Visualisation of antibody binding used the
31 Envision™ HRP-conjugated polymer system (DAKO).
32
33
34
35
36
37
38
39
40

41 Generation of brain maps

42
43 Photomicrographs of HE stained sections were captured on a Leica DM4000B bright field
44 microscope using a Leica DC500 camera. Using Photoshop 5 (Adobe), maps were generated
45 to allow comparison of similar levels.
46
47

48 Cajal-Retzius cell counts

49
50 The number of Cajal-Retzius (CR) cells were counted at two brain levels – the rostral cortex,
51 at the level of the corpus callosum; and the caudal cortex, at the level of the hippocampus.
52 To ensure consistency, levels were matched using appropriate anatomical landmarks. The
53 number of CR cells in the cortex were counted in each section. For each mouse, three serial
54 reelin-stained sections (5µm apart) were counted at rostral and caudal levels, and the mean
55
56
57
58
59
60

1
2
3 number of CR cells per section was calculated. Values were compared using a one way
4 ANOVA with Dunnett's multiple comparisons.
5
6
7
8
9
10
11
12
13
14
15
16
17
18
19
20
21
22
23
24
25
26
27
28
29
30
31
32
33
34
35
36
37
38
39
40
41
42
43
44
45
46
47
48
49
50
51
52
53
54
55
56
57
58
59
60

Results

Lesions within the cortex of FKRP^{KD} mice follow a rostrocaudal gradient; FKRP^{KD} mice exhibit the most severe brain phenotype and Large^{myd} mice the mildest.

In FKRP^{KD}, Pomgnt1_{null} and Large^{myd} mice, the rostral cortex (overlying the olfactory lobes), was disrupted. In FKRP^{KD} mice, this was characterised by a complete absence of laminar organisation, with no obvious structure to the cortical plate, and **apparent fusion of the interhemispheric fissure**. In Pomgnt1_{null} mice, as in the FKRP^{KD}, **this could be indicative of non-cleavage of the prosencephalon**. However, previous reports in other dystroglycanopathy models show that the hemispheres develop independently (60). In contrast to FKRP^{KD} mice, **some cortical plate structure, subjacent to a substantial, disorganised, extracortical layer, was apparent in the Pomgnt1_{null} mice**. Large^{myd} mice at this level were phenotypically distinct - the cortical hemispheres were separate, and multifocal defects were present, with migration of neurons and glial cells through into a narrow, extracortical layer (Figure 1A-D).

At the level of the corpus callosum, **apparent** fusion of the cortical hemispheres was still evident in FKRP^{KD} and Pomgnt1_{null} mice. In both FKRP^{KD} and Pomgnt1_{null} mice, disorganisation was more pronounced laterally. Similar to the more rostral cortex, Large^{myd} mice exhibited focal disorganisation in the cortical plate, with heterotopic neuronal and glial cells forming a narrow, subarachnoid extracortical layer (Figure 1E-H). In addition, examination of higher magnification images at this level (Figure 2) shows that normal leptomeningeal architecture is substantially disrupted in FKRP^{KD} and Pomgnt1_{null} mice. In wild type mice, the leptomeninges are readily apparent, comprising the superficial arachnoid mater, the subarachnoid space (containing the subarachnoid vessels) and the pia mater. In FKRP^{KD} and Pomgnt1_{null} mice, and to a lesser degree, Large^{myd} mice, there was little, if any distinction between these layers. The arachnoid was apparent at the cortical surface, and vessels were encompassed by heterotopic neurons and glial cells within the extracortical layer. The pia was not apparent in FKRP^{KD} and Pomgnt1_{null} mice (Figure 2).

At the level of the hippocampus, in FKRP^{KD} mice the cortical plate was more established towards the midline, than observed at more rostral levels of the cortex, although lateral aspects of the cortex were still extensively disrupted. In Pomgnt1_{null} mice at this level, the cortex was more organised laterally. Large^{myd} mice continued to exhibit the focal defects in

1
2
3 the cortical plate and the narrow extracortical layer present elsewhere in the cortex.
4 Dilation of the lateral ventricles (hydrocephalus) was present in a proportion of FKRP^{KD} (3/5)
5 and, less markedly, in Pomgnt1_{null} mice (2/5) at this time point, but was not observed in
6 Large^{myd} mice or wild type controls (Figure 1I-L). The dentate gyrus of the hippocampus was
7 disrupted in a subset (2/5) of FKRP^{KD} mice (Figure 3). Despite reports of disruption to the
8 hippocampus in adult Large^{myd} and another strain of Pomgnt1^{-/-} mice in the literature (34,
9 47), lesions were not identified in these strains at P0 in the current study.

10
11
12 The inferior and superior colliculi, were disrupted in all three lines of mice. Lesions in
13 Pomgnt1_{null} and Large^{myd} mice were characterised by focal defects with obliteration of the
14 subarachnoid space by heterotopic neuroglial cells. In FKRP^{KD} mice, there was some
15 organisation in the midline, but laterally, substantial defects in the pia enabled large
16 numbers of cells to form a prominent subarachnoid layer (Figure 1M-P; Figure 4).

17
18 Subtle cerebellar lesions, characterised by disruption to the external granule cell layer, were
19 present in 2/5 FKRP^{KD} mice and 1/5 Pomgnt1_{null} mice. Cerebellar lesions were not observed
20 in Large^{myd} mice (Figure 1M-P), however sagittal sections may allow better assessment of
21 cerebellar pathology.

22
23 Distinct patterns in lesion location/severity were observed; excluding the olfactory lobes of
24 the brain, the FKRP^{KD} and Pomgnt1_{null} mice showed rostrocaudal and lateromedial gradient
25 in the severity of cortical lesions, with the greatest degree of dyslamination in the rostral
26 and lateral aspects of the cortex. Despite the similarities in lesion localisation, the brain
27 phenotype was most substantial in FKRP^{KD} mice. Contrary to the other models,
28 Large^{myd} mice exhibited lesions of similar character and severity throughout the cortex and
29 midbrain (Figure 1).

30
31
32 Disruption to the radial glial scaffold is present in all of the mouse models of
33 dystroglycanopathy, but the glia limitans is most extensively disrupted in FKRP^{KD} mice.

34
35 In wild type mice elongate BLBP-positive processes extended to the surface of the brain,
36 where there was diffuse, continuous subpial staining of the radial glial end feet, which form
37 the glia limitans (Figure 5A. A, E, I, M).

38
39 In FKRP^{KD} mice, staining in the ventricular zone was similar to that observed in wild type
40 mice, however, radial glial processes were often haphazardly arranged, there was no subpial

1
2
3 staining (complete disruption of the glia limitans) and scattered BLBP-positive foci (radial glial
4 processes) were present within the disorganised cortical plate and extra cortical layer. The
5 tectum was less affected than the cortex, but significant abnormalities were still apparent.
6 Although relatively organised centrally and dorsomedially, discontinuous laminar staining
7 was apparent more laterally and large numbers of heterotopic neurons and glial cells were
8 present superficial to the glia limitans, expanding the sub arachnoid space (Figure 5A. B, F, J,
9 N).

10
11
12 In $Pomgnt1_{null}$ mice, disruption to the glia limitans was still substantial, but there remained
13 some foci of laminar staining (superficial to more organised areas of the cortical plate). In
14 the rest of the cortex, and in the substantial extracortical layer present above these laminar
15 foci of displaced glia limitans, were scattered BLBP-positive areas, similar to those observed
16 in the $FKRP^{KD}$ (radial glial processes). In the tectum, there was relatively little disruption to
17 the laminar architecture, but multifocally, BLBP staining was discontinuous, and neuroglial
18 cells were seen extending through the defects and expanding the subarachnoid space
19 (Figure 5A. C, G, K, O)

20
21
22 In the cortex of $Large^{myd}$ mice, the glia limitans was largely continuous, although separated
23 from the arachnoid by heterotopic neurons and glial cells. Multifocally there were defects in
24 the glia limitans, which were associated with disorganisation of the underlying cortical plate,
25 and in these areas, neurons and glial cells were visible migrating through the defects
26 expanding the subarachnoid space and forming a narrow extracortical layer. The glia
27 limitans in the tectum of $Large^{myd}$ mice displayed multifocal discontinuities in BLBP staining
28 associated with migration of neurons and glial cells through into the subarachnoid space to
29 form an extracortical layer (Figure 5A. D, H, L, P).

30
31
32 These findings indicate that there are substantial differences in the degree of disruption to
33 the glia limitans between the different mouse models which correlates with the overall
34 severity of the brain phenotype. Disruption was most pronounced in $FKRP^{KD}$ mice and
35 mildest in $Large^{myd}$ mice. Pan laminin labelling to show the location of the glial limitans is
36 shown in Figure 5B.

Expression of the IIH6 epitope of alpha dystroglycan

Expression of the IIH6 epitope of alpha dystroglycan was widespread in wild type mice (Figure 6). In addition to intense sarcolemmal staining in muscle, and fine laminar immunoreactivity at the pial basement membrane, there was intense staining of the basement membrane of blood vessels within the brain and the choroidal epithelium.

Of the dystroglycanopathy models examined, *Pomgnt1^{null}* mice showed the most pronounced, diffuse loss of IIH6 immunoreactivity. Loss of immunoreactivity was complete and all tissues examined were immunonegative.

In *FGRP^{KD}* mice a small, residual amount of sarcolemmal IIH6 immunoreactivity was observed within some, but not all, muscle groups. Immunolabelling was much less intense than that seen in wild type mice stained concurrently. Muscle types which continue to exhibit some sarcolemmal staining included the tongue, masticatory and laryngeal muscles. Interestingly, IIH6 immunoreactivity was not observed at the sarcolemma of subcutaneous muscles or extraocular muscles. Immunolabelling of the pial basement membrane and the basement membrane of the choroidal epithelium was absent.

In *Large^{myd}* mice, IIH6 immunolabelling was not apparent at the pia, similar to the *Pomgnt1^{null}* and the *FGRP^{KD}* mice. However, labelling of a similar distribution and intensity to that observed wild type mice was observed at the choroidal epithelium. In addition, in *Large^{myd}* mice, IIH6 immunolabelling was observed in multiple other epithelial structures, including the skin, developing tooth, salivary gland, choroidal epithelium and respiratory epithelium.

Mislocalisation of Cajal-Retzius cells in mouse models of dystroglycanopathy

Cajal-Retzius cells arise early in brain development and are key to the ordered migration of neurons within the cortex. They produce reelin - an extracellular glycoprotein which has roles in neuronal migration, radial glial differentiation and providing a "stop signal" to prevent over migration of neurons (54).

In wild type mice, Cajal-Retzius (CR) cells were present multifocally within the superficial molecular layer, orientated parallel to the surface. However, in *FGRP^{KD}* mice the majority of CR cells were located around the anterior cerebral artery. Scattered CR cells were present

1
2
3 within the disorganised cortical plate. Only rarely were CR cells apparent in more lateral
4 aspects of the cortex. In *Pomgnt1_{null}* mice, there was still some clustering of CR cells around
5 the anterior cerebral artery, but a larger proportion of cells extended away from the
6 midline, although they were still organised randomly and within the extracortical layer. In
7
8
9
10 *Large^{myd}* mice, CR cell localisation was more orderly, and although often CR cells were
11 present within the extracortical layer, they assumed the tangential orientation and the
12 discontinuous, laminar staining pattern of the wild type in some areas (Figure 7, A-H).

13
14
15
16 Cell counts identified a statistically-significant decrease in the number of CR cells in the
17 rostral cortex (level of the corpus callosum) in *FKRP^{KD}* and *Pomgnt1_{null}* mice ($p = 0.0002$ and
18 $p = 0.0017$, respectively). In *FKRP^{KD}* mice, there was a concurrent, statistically-significant (p
19 $= 0.046$) increase in the number of CR cells at the level of the hippocampus. In *Large^{myd}*
20 mice, there was no difference in the number of CR cells (when compared with wild type
21 mice) at either level (Figure 7I, J). These findings may suggest either a local (failure of
22 migration) or total (failure of differentiation/increased loss) decrease in the number of CR
23 cells in the cortex.
24
25
26
27
28
29
30

31 Discussion

32
33 *FKRP*, *POMGNT1* and *LARGE* are demonstrated or putative glycosyltransferases involved in
34 the post-translational modification of alpha dystroglycan (7, 10, 12, 25, 50, 79, 88). They are
35 located within the Golgi apparatus, and are hypothesised to work sequentially, with each
36 involved in the addition of a separate sugar moiety (11, 21, 38, 42, 88). They represent
37 three of the 18 genes currently implicated in the dystroglycanopathies, mutations in which
38 result in the hypoglycosylation of alpha dystroglycan (5, 6, 10, 13, 14, 44, 45, 50, 51, 66, 73,
39 78-81, 83, 84, 87, 88). At the severe end of the dystroglycanopathy spectrum (*WWS* and
40 *MEB*), patients exhibit substantial structural brain abnormalities, including neuronal
41 migration defects (manifest as pachygyria or cobblestone lissencephaly), hydrocephalus and
42 cerebellar defects (18).
43
44
45
46
47
48
49
50

51 *FKRP^{KD}* and *Pomgnt1_{null}* brain lesions exhibit a rostrocaudal and mediolateral gradient in 52 severity

53
54 There was a substantial variation in brain phenotype between the *FKRP^{KD}*, *Pomgnt1_{null}* and
55 *Large^{myd}* models, to the degree that the models could be distinguished based on
56 morphology alone. This is consistent with reports from Devisme et al. (16), who found that
57
58
59
60

1
2
3 morphological classification of neuropathologic findings in fetuses with cobblestone
4 lissencephaly enabled accurate orientation of genetic screening, and indicating that the
5 mouse models largely provide a good representation of the human disease (16).
6
7

8
9 Mice from all strains exhibited distinct patterns of lesions within the brain, which varied
10 according to the mutation. FKR^{KD} and Pomgnt1_{null} mice exhibited a rostrocaudal gradient
11 in the severity of brain lesions, with lesions most pronounced in the rostral cortex and
12 progressively milder more caudally. Additionally, there were differences mediolaterally,
13 with cortical organisation greatest towards the midline, and disruption extending laterally.
14 Unlike the other models examined, Large^{myd} mice did not exhibit this gradient of lesions –
15 defects in the Large^{myd} were multifocal and present throughout the brain.
16
17
18
19
20
21

22 Although a gradient of lesion severity has not been previously reported cases of
23 cobblestone lissencephaly in patients, specific lesion localisation is reported in other human
24 neuronal migration defects. Loss of function mutations in the G-protein coupled receptor
25 56 (GPR56) in patients is associated with the autosomal recessive brain abnormality bilateral
26 frontoparietal polymicrogyria (BFFP), in which a neuronal migration defect is isolated to the
27 frontal and parietal lobes of the brain (15). A gradient of lesions is also observed in cases of
28 classical lissencephaly. *LIS1* mutations produce lesions which are more severe in the
29 occipital lobe (posterior-predominant), whereas those produced by *DCX1* mutations are
30 more severe in the frontal lobes (anterior-predominant) (63, 67). The mechanisms
31 underlying the specific lesion localisation in BFFP or classical lissencephaly are unknown,
32 although in the case of classical lissencephaly it is believed to be due to Dcx and Lis1
33 having distinct, but related roles in signal transduction pathways (63).
34
35
36
37
38
39
40
41
42
43

44 Previously, there has been the suggestion of a medial-lateral gradient in lesion severity in
45 conditional dystroglycan null mice that corresponds to the time point at which dystroglycan
46 is lost (70). In Nestin cre-DG null mice, where there is deletion of dystroglycan from around
47 E10.5, loss of lamination and neuroglial heterotopia extend through to the lateral cortex and
48 pyriform lobe; whereas in GFAP cre-DG null mice, in which dystroglycan is deleted around
49 E13.5, lesions are focal and present only in the medial cortex (70). The differences in lesion
50 gradient observed in FKR^{KD}, Pomgnt1_{null} and Large^{myd} mice may therefore represent
51 temporal differences in the requirement for these proteins, or in the case of the Large^{myd},
52 may suggest the ability of Large homolog Large2 to compensate for the loss of Large early in
53
54
55
56
57
58
59
60

1
2
3 development. The latter point is of particular relevance as in this work, immunolabelling for
4 the I1H6 epitope of alpha dystroglycan revealed continued expression of glycosylated alpha
5 dystroglycan in the choroid plexus of this model.
6
7

8
9
10 The degree of Cajal-Retzius cell disruption is correlated with the severity of the brain lesions
11

12
13
14 In FKR^{KD}, Pomgnt1^{null} and Large^{myd} mice, the rostrocaudal and mediolateral gradient of
15 brain lesions correlates with the degree of Cajal-Retzius cell disruption observed in each of
16 the mouse strains. The areas of the cortex with the most substantial dyslamination are
17 those with the lowest number of Cajal-Retzius cells (Figure 7). FKR^{KD} mice, which exhibit
18 the most substantial mislocalisation of Cajal-Retzius cells, also have the most pronounced
19 gradient of lesions, whereas in Large^{myd} mice, which have minimal Cajal-Retzius cell
20 mislocalisation, a gradient is not apparent. Cajal-Retzius cells are one of the earliest cell
21 populations produced in the developing brain, arising from the caudomedial pallium
22 (primarily the cortical hem) and undergoing tangential migration to occupy the marginal
23 zone of the entire cortex (52, 53).
24
25
26
27
28
29
30
31

32 Reelin is an extracellular glycoprotein produced by the Cajal-Retzius cells, and this protein
33 has a number of critical roles in brain development. Reeler mice carry a mutation in the
34 *Reln* gene which encodes reelin. These mice exhibit marked cortical disruption,
35 disorganisation and inversion of cell layers, with substantial malformation of the radial glial
36 scaffold; and patients with mutations in *RELN* exhibit pachygyria with severe cerebellar
37 hypoplasia, phenotypically similar to the lesions seen in patients with WWS and MEB (28,
38 35, 82). It has been demonstrated that reelin induces a radial glial phenotype in
39 neuroepithelial progenitors via activation of Notch-1 (41), and it arrests neuronal migration
40 and promotes normal cortical lamination by providing a stop signal through the binding of
41 $\alpha_3\beta_1$ integrin (19, 48). Reelin is also responsible for the regulation of radial glial cells – in the
42 Emx1/2 and p73 knockout mice, where there is premature loss of Cajal-Retzius cells, and in
43 animals where the Cajal-Retzius cells have been chemically ablated, there are decreased
44 numbers of radial glial cells and premature transformation of radial glial cells into astrocytes
45 (55, 71, 75).
46
47
48
49
50
51
52
53
54
55
56
57
58
59
60

1
2
3
4 The severity of disruption to the radial glial scaffold is associated with Cajal-Retzius cell
5 mislocalisation
6
7

8
9 Brain lipid binding protein (BLBP) is expressed by radial glial cells. It is a cytoplasmic protein
10 involved in fatty acid uptake, transport and metabolism (22). BLBP expression, and the
11 radial glial phenotype, is induced in neuroepithelial progenitors via reelin-mediated
12 activation of Notch-1 (41). Radial glial cells are bipolar cells with elongated processes which
13 extend from the ventricular zone to the pial basement membrane, spanning the developing
14 cortex. This provides a scaffold along which neurons migrate - an integral component of the
15 'inside out' development of the mammalian cortex (64). In addition, radial glial cells provide
16 a progenitor population (29, 61, 77). Radial glial foot processes form the glia limitans (the
17 glial limiting membrane) in the developing brain, and as such form part of the blood brain
18 barrier (64). Defects in the radial glial scaffold, either physical, chemical, or genetic;
19 produce substantial abnormalities in neuronal migration and layering, causing neuronal
20 migration defects and cobblestone lissencephaly, and recapitulate the brain lesions seen in
21 patients with WWS and MEB caused by mutations in *FKRP*, *POMGNT1* and *LARGE* (61,
22 62, 65).
23
24
25
26
27
28
29
30
31
32

33
34 In *FKRP^{KD}*, *Pomgnt1_{null}* and *Large^{myd}* mice at P0, there was disruption to the radial glial end
35 feet (glia limitans), most extensive in the *FKRP^{KD}*, which was characterised by alterations in
36 the pattern and distribution of BLBP-staining. This, alongside cortical dysplasia with
37 obliteration of the subarachnoid space, neuroglial heterotopia and the apparent fusion of
38 the interhemispheric fissure, indicate radial glial cells are substantially disrupted in all of the
39 examined models of dystroglycanopathy, but most notably in the *FKRP^{KD}*. Again, the areas of
40 most substantial disruption to glial scaffold were those with the lowest number of Cajal-
41 Retzius cells. Whilst in humans additional defects in the subpial granular layer originally
42 described by Brun may contribute to these alterations, this layer was not examined in this
43 study as it is much more developed in human than other mammals (24).
44
45
46
47
48
49
50
51

52
53 *FKRP^{KD}*, *Pomgnt1_{null}* and *Large^{myd}* mice all exhibit mislocalisation of Cajal-Retzius cells,
54 however, the relative decrease in the number of Cajal-Retzius cells in the rostral cortex, with
55 the concurrent increase in the area of the hippocampus in *FKRP^{KD}* and *Pomgnt1_{null}* mice,
56
57
58
59
60

1
2
3 suggests that there is failure of tangential migration of Cajal-Retzius cells in these models.
4 This is in marked contrast to the brain lesions observed in Large^{myd} mice.
5
6

7 Given the role Cajal-Retzius cells and reelin play in neuronal migration and the organisation
8 of the radial glia, and the correlation between the degree of Cajal-Retzius cell
9 mislocalisation and the location and severity of the brain lesions observed, this suggests that
10 Cajal-Retzius cell mislocalisation may have a significant role in the manifestation of the brain
11 phenotype. In addition, it suggests that factors affecting Cajal-Retzius cell migration may
12 underpin the pathogenesis of the structural brain defects in FKR^{KD} and Pomgnt1_{null} mice,
13 but not Large^{myd} mice. Radial glial fibres form the initial migratory microcolumns, whilst the
14 migration of inhibitory interneurons initiated prior to radial migration, forms the marginal
15 zone of the preplate which includes Cajal Retzius cells, molecular zone and subplate neurons
16 (68). Horizontal lamination in the newborn FKR^{KD} brain as detected using markers such as
17 Tbr1 and Ctip2 is clearly evident although it shows a disturbed pattern (3).
18
19
20
21
22
23
24
25
26

27 Previously, it has been hypothesised that, as disruption to the glia limitans and neuronal
28 migration defects are largely localised to the areas of the brain which undergo most
29 pronounced and rapid expansion during development. In agreement with this the brain
30 lesions in dystroglycanopathy models were reported to develop due to failure of the radial
31 glial cells to appropriately organise the basement membrane during periods of rapid cortical
32 expansion (60). This idea was strengthened by data from a Pomgnt1^{-/-} strain, whereby the
33 basement membrane was initially normal and was intact at E11.5, but abnormalities were
34 apparent by E13.5 (36). Similarly, in Nestin cre-DG null mice, in which dystroglycan was
35 knocked out from E10.5, abnormalities in the basement membrane were first apparent at
36 E13.5 (70).
37
38
39
40
41
42
43
44

45 Radial glial endfeet retraction could potentially account for the lesions observed in Large^{myd}
46 mice, in which Cajal-Retzius cells are mislocalised but do not exhibit a failure of migration.
47 However, our observations of a disruption in Cajal-Retzius cell migration in FKR^{KD} and
48 Pomgnt1_{null} mice are suggestive of a more complex pathogenesis albeit not one which
49 excludes a role for the radial glia. Indeed previous work in which the radial glial scaffold was
50 disrupted without impacting on either the meninges or basement membrane integrity
51 demonstrated a primary role for radial glia in Cajal Retzius cell localisation (43).
52
53
54
55
56
57
58
59
60

1
2
3 The mechanisms involved in the migration of Cajal-Retzius cells from their birthplace to
4 cover the marginal zone of the entire cortex are not fully understood, although the process
5 is known to be influenced by a number of factors. The leptomeninges are central to the
6 orchestration of this process, through both their physical presence and through chemokine
7 signalling via the CXCL12/CXCR4 pathway (8). Surgical, chemical or genetic disruption of the
8 leptomeninges produces Cajal-Retzius cell degeneration with pronounced disruption in
9 Cajal-Retzius cell localisation, further indicating the importance of the leptomeninges to
10 Cajal-Retzius cells (30, 40, 48, 75, 76). In addition, the leptomeninges are morphologically
11 abnormal in the mouse models of dystroglycanopathy, as identified in this study and in a
12 *Pomgnt1*^{-/-} mouse model in work by Yang et al. (85). Taken together, this implicates a role
13 for abnormalities in leptomeningeal cells in the pathogenesis of the dystroglycanopathies.
14
15
16
17
18
19
20
21
22

23 Expression of the IIH6 epitope of alpha dystroglycan varies between mouse models of
24 dystroglycanopathy
25

26 Despite the presence of significant brain phenotypes in *FGRP*^{KD}, *Pomgnt1*_{null} and *Large*^{myd}
27 mice; and published muscle and eye phenotypes in these models (1, 2, 32, 34), there was
28 significant variation in the expression of the glycoepitope of alpha dystroglycan recognised
29 by the IIH6 antibody between them. In both *FGRP*^{KD} and *Pomgnt1*_{null} mice, no IIH6
30 immunolabelling was identified in the brain.
31
32
33
34
35

36 In the brain of *Large*^{myd} mice, the IIH6 epitope was still strongly expressed at the choroid
37 plexus, despite an absence of IIH6 expression at the pia mater, and at the sarcolemma in the
38 muscle. In addition, in *Large*^{myd} mice, IIH6 continued to be expressed throughout epithelial
39 structures. *In situ* hybridisation data provided by Hewitt (personal communication),
40 identified expression of the *Large* paralogue *Large2* in the choroid plexus and in epithelial
41 structures outside of the brain. *Large2* has been identified as having the same
42 xylosyltransferase and glucuronyltransferase activities as *Large*, but with different
43 biochemical properties, most likely accounting for the difference in tissue expression
44 observed by Grewal et al. (4, 26, 39). Interestingly, despite the identification of *Large2*
45 expression at the choroid plexus by *in situ* hybridisation, expression was not observed in the
46 brain with RT-PCR, northern blot or dot blot analysis (26). The reason for the discrepancy
47 between these results is not certain, but may relate to the expression of *Large2* by a very
48 limited population of cells being “diluted” in the whole brain homogenates used for RT-PCR,
49
50
51
52
53
54
55
56
57
58
59
60

1
2
3 northern blot and dot blots. Other than the labelling at the choroid plexus, the expression of
4 the I1H6 epitope of alpha dystroglycan appeared to correlate with the expression patterns
5 reported by Grewal et al. (26), and was observed exclusively within epithelial structures.
6
7

8
9 It is not known how the retention of expression of glycosylated alpha dystroglycan in the
10 choroid plexus relates to the relatively mild brain phenotype observed in *Large*^{myd} mice.
11 Studies of embryonic development in *Large*^{myd} mice have not been published, therefore it is
12 not known whether the deficiency in *Large* is compensated for by the up regulation of
13 *Large2* at earlier developmental time points.
14
15
16

17
18 This work clearly demonstrates that there is substantial variation in the brain phenotype
19 between mouse models of the dystroglycanopathies, indicating that a “one-model-fits-all”
20 approach to the investigation of underlying mechanisms is not appropriate, and reiterating
21 the importance of both careful model selection, and the use of multiple mouse models, in
22 investigative work. Since Cajal-Retzius cells typically respond to cues originating from the
23 meninges, our results suggest that whilst cortical defects in *Large*^{myd} mice are consistent
24 with a disturbance of the radial glial scaffold as previously reported, the more severe
25 phenotype observed in *FKRP*^{KD} and *Pomgnt1*_{null} mice imply additional defects in the
26 meninges. Whilst the subplate was not included in the present study, it is comprised of early
27 born neurons that are of substantial interest to the present work in that they are generated
28 around the same time as the Cajal Retzius cells. Indeed the subplate is a highly dynamic
29 structure the transcriptomic profile of which suggests a number of intriguing roles which
30 change through development. Future work in this area might profit from an analysis of this
31 heterogenous cell population (33).
32
33
34
35
36
37
38
39
40
41
42
43

44 It should be noted that whilst the present paper focuses on the role of the pial basement
45 membrane in cortical development, neuron:neuron and neuron:glial interactions also play a
46 key role in orchestrating development of the cortex. These interactions are mediated by
47 integrins, N-cadherin, gap junction proteins together with a number of signaling pathways
48 some of which are downstream of reelin (72). Future work may benefit particularly from a
49 more detailed exploration of adhesion receptor trafficking which underlies the migration of
50 all cells and laminin internalisation in the secondary dystroglycanopathies, the latter of
51 which has been shown to utilize dystroglycan in cancer cells (46).
52
53
54
55
56
57
58
59
60

1
2
3 In summary our observations implicate gene specific differences in the pathogenesis of
4 brain lesions in this group of disorders. Further work is required to identify whether a defect
5 in another cell type (such as the leptomeningeal cells) contributes to these phenotypes.
6
7

8
9 HSB and SCB designed the study and wrote the paper, HSB, JLW and MH performed the
10 experiments and analysed the data.
11

12
13 The authors confirm that they have no conflict of interests either personally or financially.
14

15 SCB gratefully acknowledges the support of the Muscular Dystrophy Association (USA) and
16 Association contres les myopathies (AFM). HSB is supported by the Royal Veterinary College.
17
18
19
20
21
22
23
24
25
26
27
28
29
30
31
32
33
34
35
36
37
38
39
40
41
42
43
44
45
46
47
48
49
50
51
52
53
54
55
56
57
58
59
60

1
2
3 **Figure 1:** There are substantial histopathological differences in the brain phenotype in FKRP^{KD},
4
5 Pomgnt1_{null} and Large^{myd} mice at P0
6
7

8 A, B, C, D. Olfactory lobes and rostral cortex. In the wild type (A), the organised neocortex is
9
10 apparent dorsal to the olfactory lobes. In the FKRP^{KD} and Pomgnt1_{null} mice (B and C, respectively)
11
12 the olfactory lobes (OL) are normal, but there is fusion of the cortical hemispheres (arrow head) and
13
14 substantial dyslamination of the rostral neocortex. Cortical disorganisation is most apparent in the
15
16 FKRP^{KD}. In the Large^{myd} (D), the olfactory lobes are again normal. In these mice the cortical
17
18 hemispheres remain distinct at this level, but do exhibit disruption in lamination.
19

20
21 E, F, G, H. Cortex around the level of the corpus callosum. The cortical plate is distinct, and overlain
22
23 by the cell-poor marginal zone in wild type mice (E). In the FKRP^{KD} (F), the cortex is completely
24
25 disorganised, and the cortical plate is indistinct. The Pomgnt1_{null} and Large^{myd} mice (G and H,
26
27 respectively) have well defined cortical plates, but these are overlain by a cell-dense, subarachnoid,
28
29 extracortical layer, which is more pronounced in the Pomgnt1_{null} mice. In Pomgnt1_{null} mice, the
30
31 lateral cortex is more disorganised than the medial cortex (fine arrow).
32
33

34
35 I, J, K, L. Cortex around the level of the hippocampus. At this level, the FKRP^{KD}, POMGnT1_{null} and
36
37 Large^{myd} mice (J, K and L, respectively) all exhibit **incomplete formation** of the interhemispheric
38
39 fissure with interdigitation of neurons from opposing cortical plates. In the FKRP^{KD}, the remnants of
40
41 the cortical plate are apparent medially, with dyslamination increasing laterally (J, fine arrow). There
42
43 is ventricular dilation in the FKRP^{KD} and, to a lesser extent the POMGnT1_{null} (*). In addition, there is
44
45 some rarefaction of the subventricular zone in the FKRP^{KD} only.
46
47

48
49 M, N, O, P. Tectum and cerebellum. There is disorganisation of the inferior colliculus, most marked
50
51 in the FKRP^{KD} (star). There is some disruption to the granule cell layer of the cerebellum in the
52
53 FKRP^{KD} and POMGnT1_{null} (N and O, respectively; bold arrow), when compared to the wild type (M).
54
55 The cerebellum in the Large^{myd} (P) does not appear to be affected at this time point.
56
57
58
59
60

1
2
3 HE. Bars represent 400µm. N = neocortex; OL = olfactory lobes; H = hippocampus; LV = lateral
4
5 ventricles; T = tectum; C = cerebellum.
6
7

8 **Figure 2:** Neocortex at the level corpus callosum.

9
10 Neocortex at the level of the corpus callosum. There is consistent fusion of the cortical hemispheres
11
12 in the FKRP^{KD} (B, F) and the Pomgnt1^{null} (C, G), with interdigitation of neurons from opposing cortical
13
14 plates. This is not consistently observed in the Large^{myd} at this level (D, H). The degree of
15
16 disorganisation of the cortical plate varies between models. The cortical plate is inapparent in FKRP^{KD}
17
18 mice, and no marginal zone is observed. In Pomgnt1^{null} mice the marginal zone and cortical plate are
19
20 apparent beneath a substantial extracortical layer. The Large^{myd} mice demonstrate a relatively
21
22 organised cortical plate, but multifocally neurons from the cortical plate are apparent migrating
23
24 through the marginal zone and the pial basement membrane and running subjacent and tangential
25
26 to the arachnoid to form a narrow extra cortical layer (fine arrows). The tramline appearance of the
27
28 normal meninges is not present in FKRP^{KD}, Pomgnt1^{null} and is only multifocally observed in Large^{myd}
29
30 mice.
31
32

33
34 HE. A-D – bars represent 400µm; E-F – bars represent 200µm. LV = lateral ventricles; M =
35
36 leptomeninges; MZ = marginal zone; CP = cortical plate; ECL = extra cortical layer.
37
38

39 **Figure 3:** Neocortex at the level of the hippocampus.

40
41 For comparison wild type mice are shown in A,E and I. In the neocortex at the level of the
42
43 hippocampus, laminar architecture is most disrupted in FKRP^{KD} mice, (B,F,J) and to a lesser extent,
44
45 Pomgnt1^{null} mice (C,G,K). The Large^{myd} mice are least affected (D,H,L). Although the cortex is more
46
47 organised at this level than rostrally in FKRP^{KD} mice, there is a distinct lateromedial gradient in
48
49 severity of lesions (bold arrow). There is interdigitation of opposing cortical plates in all mice,
50
51 including the Large^{myd} at this level. Disruption to the hippocampus, particularly the dentate gyrus,
52
53 was present in a proportion of the FKRP^{KD} mice (arrowheads), but was not observed in either the
54
55 Pomgnt1^{null} or the Large^{myd}.
56
57
58
59
60

HE. A-D - bars represent 400µm; E-H - bars represent 200µm; I-L – bars represent 100µm. N = neocortex; H = hippocampus; DG = dentate gyrus; ECL = extracortical layer; CP = cortical plate.

Figure 4: Midbrain at the level of the inferior colliculus

Midbrain: Disorganisation is apparent in the superior and inferior colliculi. For comparison wild type mice are shown in A and E. At this level, the phenotype is similar in the *Pomgnt1_{null}* (C, G) and *Large^{myd}* mice (D,H), with multifocal defects in the pial basement membrane allowing migration of neuron and glial cells into the subarachnoid space (chevrons). In the *FKRP^{KD}* (B, F) there are appear to be more substantial defects in the pial basement membrane laterally (star), allowing a substantial layer of neurons to form above the colliculus itself.

HE. M-P – bars represent 200µm; m-p – bars represent 100µm. T = tectum; V = ventricle.

Figure 5A: Immunohistochemical evaluation of the glia limitans.

A-H. Cortex. BLBP staining of radial glial cells and the glia limitans. The bold arrow indicates the glia limitans. In wild type mice, the glia limitans is apparent as a continuous subpial layer (A, E). The glia limitans is disrupted, to varying degrees, in the *FKRP^{KD}*, *Pomgnt1_{null}* and *Large^{myd}* (B, C and D respectively). Higher power images show that in the *FKRP^{KD}* (F) mislocalised radial glial foot processes can be observed scattered randomly throughout the cortex. In *Pomgnt1_{null}* mice (G), multifocal, discontinuous areas of laminar staining are present subjacent to a substantial extracortical layer. *Large^{myd}* mice (H) have a relatively well formed glia limitans. There are multifocal small defects with migration of the neuroglial cells through the deficits into a narrow extra cortical layer. **Insets contained within E,F,G,H show higher power magnifications.** A-D – bar represents 400µm; E-H – bar represents 100µm. N = neocortex; VZ = ventricular zone.

I-P. Tectum (inferior colliculus). There is disruption to the glia limitans in the midbrain of the *FKRP^{KD}*, the *Pomgnt1_{null}* and the *Large^{myd}* (J, K and L, respectively). The *Pomgnt1_{null}* and the *Large^{myd}* are histologically similar at this site – there are multifocal defects in the glial limitans (fine arrows), with migration of neuroglial cells through the defects to expand the subarachnoid space (O, P). In

1
2
3 addition to multifocal defects, the FKRP^{KD} exhibits disorganisation laterally – laminar BLBP-positive
4
5 foci (radial glial processes) are apparent towards the midline not laterally (star), and there is
6
7 expansion of the subarachnoid space by a substantial population of neuroglial cells (N). I-L –bar
8
9 represents 400µm; M-P – bar represents 200µm. T = tectum.

10
11
12 **Figure 5B: Immunohistochemical staining for pan laminin in mouse models of dystroglycanopathy**

13
14 A-D. Pan laminin staining of the cortex highlighting the location of the glia limitans (see arrow) in the
15
16 wild type (A), FKRP^{KD} (B), Pomgnt1_{null} (C) and Large^{myd} (D). Higher power images are shown in E-H. A-
17
18 D – bar represents 200µm; E-H – bar represents 100µm.

19
20
21
22
23
24 **Figure 6: Immunohistochemical staining for the IIH6 epitope of glycosylated alpha dystroglycan in**
25
26 mouse models of dystroglycanopathy

27
28 A, B, C, D. Lateral head sections stained with IIH6 antibody. The skin, pial basement membrane and
29
30 inner limiting membrane of the eye exhibit strong staining in the wild type, in addition to
31
32 sarcolemmal staining present in the extraocular and subcutaneous muscles (A). Staining of all of
33
34 these structures is absent in FKRP^{KD} and Pomgnt1_{null} mice (B, C). In Large^{myd} mice (D), the skin
35
36 remains immunopositive, but staining is absent in other tissues. Bars represent 400µm.

37
38
39
40 E, F, G, H. IIH6 staining in the brain at the level of the hippocampus. In the WT (E), the basement
41
42 membrane of choroid plexus is strongly immunopositive and there is a narrow, laminar staining
43
44 pattern at the pial basement membrane (arrowheads). In the FKRP^{KD} and Pomgnt1_{null} mice (F and G,
45
46 respectively), no staining is apparent. In the Large^{myd}, the basement membrane of the choroid
47
48 plexus is strongly immunopositive, but there is no staining at the pial basement membrane. Bars
49
50 represent 200µm.

51
52
53 HS = haired skin; SCM = subcutaneous muscle; EOM = extraocular muscle; E = eye; N = neocortex; OL
54
55 = olfactory lobe; NC = nasal cavity; CP = choroid plexus.

Figure 7: Mislocalisation of the CR cells

Immunohistochemical staining of the Cajal-Retzius cells with an antibody to reelin, at the level of the corpus callosum (A, C, E, G – bar represents 200µm) and at the hippocampus (B, D, F, H – bar represents 400µm). In wild type mice there are multifocal, tangentially-orientated, reelin-positive Cajal-Retzius cells which form an intermittent, single-cell layer within the marginal zone (A, B). Large numbers of CR cells are present at the hippocampus. In FKRP^{KD} mice, there is a significant decrease in the number of reelin-positive cells at the level of the corpus callosum (C). Those present are disorganised, haphazardly orientated and predominantly clustered around the anterior cerebral artery. At the level of the hippocampus, more normally distributed and orientated CR cells appear to be associated with more ordered areas of the cortical plate (D). In the POMGnT1null mice (E) there is less clustering of the CR cells around the anterior cerebral artery. CR cells extend further laterally, although are randomly distributed within the extracortical layer. Again, CR cell distribution appears more normal at the level of the hippocampus (F). In the Large^{myd} (G) CR cells are orientated predominantly transversely (as in the wild type) but are overlain by a narrow extracortical layer, rostrally. There is some disruption in the midline at the level of the hippocampus, in areas of fusion of opposing cortical plates (H). a-d. Higher magnification views of the cortex at the level of the corpus callosum, lateral to the interhemispheric fissure (bars represent 100µm).

At the level of the corpus callosum (I) there is a statistically-significant decrease in the number of CR cells in FKRPKD ($P = 0.0002$) and Pomgnt1null mice ($P = 0.0017$), relative to wild type mice (one way ANOVA with Dunnett's multiple comparisons). This is not observed in Large^{myd} mice ($P = 0.986$). At the level of the hippocampus (J) in FKRPKD there is a statistically-significant increase in the number of CR cells relative to wild type ($P = 0.046$) but no statistically-significant differences in the number of CR cells in either Pomgnt1null or Large^{myd} mice relative to wild type ($P = 0.304$ and $P = 0.930$, respectively).

1. Ackroyd MR, Skordis L, Kaluarachchi M, Godwin J, Prior S, Fidanboylyu M, Piercy RJ, Muntoni F, Brown SC (2009) Reduced expression of fukutin related protein in mice results in a model for fukutin related protein associated muscular dystrophies. *Brain*.132(Pt 2):439-51.
2. Ackroyd MR, Whitmore C, Prior S, Kaluarachchi M, Nikolic M, Mayer U, Muntoni F, Brown SC (2011) Fukutin-Related Protein Alters the Deposition of Laminin in the Eye and Brain. *The Journal of Neuroscience*.31(36):12927-35.
3. Ackroyd MR, Whitmore C, Prior S, Kaluarachchi M, Nikolic M, Mayer U, Muntoni F, Brown SC (2011) Fukutin-related protein alters the deposition of laminin in the eye and brain. *JNeurosci*.31(36):12927-35.
4. Ashikov A, Buettner FF, Tiemann B, Gerardy-Schahn R, Bakker H (2013) LARGE2 generates the same xylose- and glucuronic acid-containing glycan structures as LARGE. *Glycobiology*.23(3):303-9.
5. Barone R, Aiello C, Race V, Morava E, Foulquier F, Riemersma M, Passarelli C, Concolino D, Carella M, Santorelli F, Vleugels W, Mercuri E, Garozzo D, Sturiale L, Messina S, Jaeken J, Fiumara A, Wevers RA, Bertini E, Matthijs G, Lefeber DJ (2012) DPM2-CDG: a muscular dystrophy-dystroglycanopathy syndrome with severe epilepsy. *Annals of neurology*.72(4):550-8.
6. Beltran-Valero de Bernabe D, Currier S, Steinbrecher A, Celli J, van Beusekom E, van der Zwaag B, Kayserili H, Merlini L, Chitayat D, Dobyns WB, Cormand B, Lehesjoki AE, Cruces J, Voit T, Walsh CA, van Bokhoven H, Brunner HG (2002) Mutations in the O-mannosyltransferase gene POMT1 give rise to the severe neuronal migration disorder Walker-Warburg syndrome. *American journal of human genetics*.71(5):1033-43.
7. Beltran-Valero de Bernabe D, Voit T, Longman C, Steinbrecher A, Straub V, Yuva Y, Herrmann R, Sperner J, Korenke C, Diesen C, Dobyns WB, Brunner HG, van Bokhoven H, Brockington M, Muntoni F (2004) Mutations in the FKR gene can cause muscle-eye-brain disease and Walker-Warburg syndrome. *Journal of medical genetics*.41(5):e61.
8. Borrell V, Marin O (2006) Meninges control tangential migration of hem-derived Cajal-Retzius cells via CXCL12/CXCR4 signaling. *Nature neuroscience*.9(10):1284-93.
9. Bouchet C, Gonzales M, Vuillaumier-Barrot S, Devisme L, Lebizec C, Alanio E, Bazin A, Bessieres-Grattagliano B, Bigi N, Blanchet P, Bonneau D, Bonnieres M, Carles D, Delahaye S, Fallet-Bianco C, Figarella-Branger D, Gaillard D, Gasser B, Guimiot F, Joubert M, Laurent N, Liprandi A, Loget P, Marcocelles P, Martinovic J, Menez F, Patrier S, Pelluard-Nehme F, Perez MJ, Rouleau-Dubois C, Triau S, Laquerriere A, Encha-Razavi F, Seta N (2007) Molecular heterogeneity in fetal forms of type II lissencephaly. *Human mutation*.28(10):1020-7.
10. Brockington M, Blake DJ, Prandini P, Brown SC, Torelli S, Benson MA, Ponting CP, Estournet B, Romero NB, Mercuri E, Voit T, Sewry CA, Guicheney P, Muntoni F (2001) Mutations in the fukutin-related protein gene (FKRP) cause a form of congenital muscular dystrophy with secondary laminin alpha2 deficiency and abnormal glycosylation of alpha-dystroglycan. *American journal of human genetics*.69(6):1198-209.
11. Brockington M, Torelli S, Prandini P, Boito C, Dolatshad NF, Longman C, Brown SC, Muntoni F (2005) Localization and functional analysis of the LARGE family of glycosyltransferases: significance for muscular dystrophy. *Hum Mol Genet*.14(5):657-65.
12. Brockington M, Yuva Y, Prandini P, Brown SC, Torelli S, Benson MA, Herrmann R, Anderson LV, Bashir R, Burgunder JM, Fallet S, Romero N, Fardeau M, Straub V, Storey G, Pollitt C, Richard I, Sewry CA, Bushby K, Voit T, Blake DJ, Muntoni F (2001) Mutations in the fukutin-related protein gene (FKRP) identify limb girdle muscular dystrophy 2I as a milder allelic variant of congenital muscular dystrophy MDC1C. *Hum Mol Genet*.10(25):2851-9.
13. Buysse K, Riemersma M, Powell G, van Reeuwijk J, Chitayat D, Roscioli T, Kamsteeg EJ, van den Elzen C, van Beusekom E, Blaser S, Babul-Hirji R, Halliday W, Wright GJ, Stemple DL, Lin YY, Lefeber DJ, van Bokhoven H (2013) Missense mutations in beta-1,3-N-acetylglucosaminyltransferase 1 (B3GNT1) cause Walker-Warburg syndrome. *Hum Mol Genet*.22(9):1746-54.

14. Carss KJ, Stevens E, Foley AR, Cirak S, Riemersma M, Torelli S, Hoischen A, Willer T, van Scherpenzeel M, Moore SA, Messina S, Bertini E, Bonnemann CG, Abdenur JE, Grosman CM, Kesari A, Punetha J, Quinlivan R, Waddell LB, Young HK, Wraige E, Yau S, Brodd L, Feng L, Sewry C, MacArthur DG, North KN, Hoffman E, Stemple DL, Hurler ME, van Bokhoven H, Campbell KP, Lefeber DJ, Consortium UK, Lin YY, Muntoni F (2013) Mutations in GDP-mannose pyrophosphorylase B cause congenital and limb-girdle muscular dystrophies associated with hypoglycosylation of alpha-dystroglycan. *Am J Hum Genet.*93(1):29-41.
15. Chiang NY, Hsiao CC, Huang YS, Chen HY, Hsieh IJ, Chang GW, Lin HH (2011) Disease-associated GPR56 mutations cause bilateral frontoparietal polymicrogyria via multiple mechanisms. *The Journal of biological chemistry.*286(16):14215-25.
16. Devisme L, Bouchet C, Gonzales M, Alanio E, Bazin A, Bessieres B, Bigi N, Blanchet P, Bonneau D, Bonnieres M, Bucourt M, Carles D, Clarisse B, Delahaye S, Fallet-Bianco C, Figarella-Branger D, Gaillard D, Gasser B, Delezoide AL, Guimiot F, Joubert M, Laurent N, Laquerriere A, Liprandi A, Loget P, Marcorelles P, Martinovic J, Menez F, Patrier S, Pelluard F, Perez MJ, Rouleau C, Triau S, Attie-Bitach T, Vuillaumier-Barrot S, Seta N, Encha-Razavi F (2012) Cobblestone lissencephaly: neuropathological subtypes and correlations with genes of dystroglycanopathies. *Brain.*135(Pt 2):469-82.
17. Dobyns WB, Kirkpatrick JB, Hittner HM, Roberts RM, Kretzer FL (1985) Syndromes with lissencephaly. II: Walker-Warburg and cerebro-oculo-muscular syndromes and a new syndrome with type II lissencephaly. *Am J Med Genet.*22(1):157-95.
18. Dobyns WB, Pagon RA, Armstrong D, Curry CJ, Greenberg F, Grix A, Holmes LB, Laxova R, Michels VV, Robinow M, et al. (1989) Diagnostic criteria for Walker-Warburg syndrome. *Am J Med Genet.*32(2):195-210.
19. Dulabon L, Olson EC, Taglienti MG, Eisenhuth S, McGrath B, Walsh CA, Kreidberg JA, Anton ES (2000) Reelin binds alpha3beta1 integrin and inhibits neuronal migration. *Neuron.*27(1):33-44.
20. Ervasti JM, Campbell KP (1993) A role for the dystrophin-glycoprotein complex as a transmembrane linker between laminin and actin. *The Journal of cell biology.*122(4):809-23.
21. Esapa CT, Benson MA, Schroder JE, Martin-Rendon E, Brockington M, Brown SC, Muntoni F, Kroger S, Blake DJ (2002) Functional requirements for fukutin-related protein in the Golgi apparatus. *Hum Mol Genet.*11(26):3319-31.
22. Feng L, Hatten ME, Heintz N (1994) Brain lipid-binding protein (BLBP): a novel signaling system in the developing mammalian CNS. *Neuron.*12(4):895-908.
23. Gee SH, Montanaro F, Lindenbaum MH, Carbonetto S (1994) Dystroglycan-alpha, a dystrophin-associated glycoprotein, is a functional agrin receptor. *Cell.*77(5):675-86.
24. Goffinet AM (2006) What makes us human? A biased view from the perspective of comparative embryology and mouse genetics. *Journal of biomedical discovery and collaboration.*1:16.
25. Grewal PK, Hewitt JE (2002) Mutation of Large, which encodes a putative glycosyltransferase, in an animal model of muscular dystrophy. *Biochimica et biophysica acta.*1573(3):216-24.
26. Grewal PK, McLaughlan JM, Moore CJ, Browning CA, Hewitt JE (2005) Characterization of the LARGE family of putative glycosyltransferases associated with dystroglycanopathies. *Glycobiology.*15(10):912-23.
27. Hara Y, Balci-Hayta B, Yoshida-Moriguchi T, Kanagawa M, Beltran-Valero de Bernabe D, Gundesli H, Willer T, Satz JS, Crawford RW, Burden SJ, Kunz S, Oldstone MB, Accardi A, Talim B, Muntoni F, Topaloglu H, Dincer P, Campbell KP (2011) A dystroglycan mutation associated with limb-girdle muscular dystrophy. *The New England journal of medicine.*364(10):939-46.
28. Hartfuss E, Förster E, Bock HH, Hack MA, Leprince P, Luque JM, Herz J, Frotscher M, Götz M (2003) Reelin signaling directly affects radial glia morphology and biochemical maturation. *Development.*130:597-4609.

- 1
- 2
- 3 29. Hartfuss E, Galli R, Heins N, Gotz M (2001) Characterization of CNS precursor subtypes and
- 4 radial glia. *Dev Biol.*229(1):15-30.
- 5 30. Hecht JH, Siegenthaler JA, Patterson KP, Pleasure SJ (2010) Primary cellular meningeal
- 6 defects cause neocortical dysplasia and dyslamination. *Ann Neurol.*68(4):454-64.
- 7 31. Henry MD, Campbell KP (1998) A role for dystroglycan in basement membrane assembly.
- 8 *Cell.*95(6):859-70.
- 9 32. Hewitt JE (2010) Investigating the Functions of LARGE: Lessons from Mutant Mice. *Methods*
- 10 *in Enzymology.*479:367-81.
- 11 33. Hoerder-Suabedissen A, Molnar Z (2015) Development, evolution and pathology of
- 12 neocortical subplate neurons. *Nature reviews Neuroscience.*16(3):133-46.
- 13 34. Holzfeind PJ, Grewal PK, Reitsamer HA, Kechvar J, Lassmann H, Hoeger H, Hewitt JE, Bittner
- 14 RE (2002) Skeletal, cardiac and tongue muscle pathology, defective retinal transmission, and
- 15 neuronal migration defects in the Large^{myd} mouse defines a natural model for glycosylation-deficient
- 16 muscle – eye – brain disorders. *Human Molecular Genetics.*11(21):2673–87.
- 17 35. Hong SE, Shugart YY, Huang DT, Shahwan SA, Grant PE, Hourihane JO, Martin ND, Walsh CA
- 18 (2000) Autosomal recessive lissencephaly with cerebellar hypoplasia is associated with human RELN
- 19 mutations. *Nat Genet.*26(1):93-6.
- 20 36. Hu H, Yang Y, Eade A, Xiong YF, Qi Y (2007) Breaches of the Pial Basement Membrane and
- 21 Disappearance of the Glia Limitans During Development Underlie the Cortical Lamination Defect in
- 22 the Mouse Model of Muscle-Eye-Brain Disease. *The Journal of Comparative Neurology.*501:168-83.
- 23 37. Ibraghimov-Beskrovnya O, Ervasti JM, Leveille CJ, Slaughter CA, Sernett SW, Campbell KP
- 24 (1992) Primary structure of dystrophin-associated glycoproteins linking dystrophin to the
- 25 extracellular matrix. *Nature.*355(6362):696-702.
- 26 38. Inamori K, Yoshida-Moriguchi T, Hara Y, Anderson ME, Yu L, Campbell KP (2012)
- 27 Dystroglycan function requires xylosyl- and glucuronyltransferase activities of LARGE.
- 28 *Science.*335(6064):93-6.
- 29 39. Inamori KI, Hara Y, Willer T, Anderson ME, Zhu Z, Yoshida-Moriguchi T, Campbell KP (2012)
- 30 Xylosyl- and glucuronyltransferase functions of LARGE in alpha-dystroglycan modification are
- 31 conserved in LARGE2. *Glycobiology.*
- 32 40. Inoue T, Ogawa M, Mikoshiba K, Aruga J (2008) Zic deficiency in the cortical marginal zone
- 33 and meninges results in cortical lamination defects resembling those in type II lissencephaly. *The*
- 34 *Journal of neuroscience : the official journal of the Society for Neuroscience.*28(18):4712-25.
- 35 41. Keilani S, Sugaya K (2008) Reelin induces a radial glial phenotype in human neural progenitor
- 36 cells by activation of Notch-1. *BMC Developmental Biology.*8(69).
- 37 42. Keramaris-Vrantsis E, Lu PJ, Doran T, Zillmer A, Ashar J, Esapa CT, Benson MA, Blake DJ,
- 38 Rosenfeld J, Lu QL (2007) Fukutin-related protein localizes to the Golgi apparatus and mutations lead
- 39 to mislocalization in muscle in vivo. *Muscle & nerve.*36(4):455-65.
- 40 43. Kwon HJ, Ma S, Huang Z (2011) Radial glia regulate Cajal-Retzius cell positioning in the early
- 41 embryonic cerebral cortex. *Developmental biology.*351(1):25-34.
- 42 44. Lefeber DJ, de Brouwer AP, Morava E, Riemersma M, Schuurs-Hoeijmakers JH, Absmanner B,
- 43 Verrijp K, van den Akker WM, Huijben K, Steenbergen G, van Reeuwijk J, Jozwiak A, Zucker N, Lorber
- 44 A, Lammens M, Knopf C, van Bokhoven H, Grunewald S, Lehle L, Kapusta L, Mandel H, Wevers RA
- 45 (2011) Autosomal recessive dilated cardiomyopathy due to DOLK mutations results from abnormal
- 46 dystroglycan O-mannosylation. *PLoS genetics.*7(12):e1002427.
- 47 45. Lefeber DJ, Schonberger J, Morava E, Guillard M, Huyben KM, Verrijp K, Grafakou O,
- 48 Evangeliou A, Preijers FW, Manta P, Yildiz J, Grunewald S, Spilioti M, van den Elzen C, Klein D, Hess D,
- 49 Ashida H, Hofsteenge J, Maeda Y, van den Heuvel L, Lammens M, Lehle L, Wevers RA (2009)
- 50 Deficiency of Dol-P-Man synthase subunit DPM3 bridges the congenital disorders of glycosylation
- 51 with the dystroglycanopathies. *American journal of human genetics.*85(1):76-86.
- 52
- 53
- 54
- 55
- 56
- 57
- 58
- 59
- 60

- 1
2
3 46. Leonoudakis D, Huang G, Akhavan A, Fata JE, Singh M, Gray JW, Muschler JL (2014)
4 Endocytic trafficking of laminin is controlled by dystroglycan and is disrupted in cancers. *J Cell*
5 *Sci.*127(22):4894-903.
6 47. Li J, Yu M, Feng G, Hu H, Li X (2011) Breaches of the pial basement membrane are associated
7 with defective dentate gyrus development in mouse models of congenital muscular dystrophies.
8 *Neurosci Lett.*505(1):19-24.
9 48. Li S, Jin Z, Koirala S, Bu L, Xu L, Hynes RO, Walsh CA, Corfas G, Piao X (2008) GPR56 regulates
10 pial basement membrane integrity and cortical lamination. *The Journal of neuroscience : the official*
11 *journal of the Society for Neuroscience.*28(22):5817-26.
12 49. Liu J, Ball SL, Yang Y, Mei P, Zhang L, Shi H, Kaminski HJ, Lemmon VP, Hu H (2006) A genetic
13 model for muscle-eye-brain disease in mice lacking protein O-mannose 1,2-N-
14 acetylglucosaminyltransferase (POMGnT1). *Mechanisms of Development.*123:228-40.
15 50. Longman C, Brockington M, Torelli S, Jimenez-Mallebrera C, Kennedy C, Khalil N, Feng L,
16 Saran RK, Voit T, Merlini L, Sewry CA, Brown SC, Muntoni F (2003) Mutations in the human LARGE
17 gene cause MDC1D, a novel form of congenital muscular dystrophy with severe mental retardation
18 and abnormal glycosylation of alpha-dystroglycan. *Hum Mol Genet.*12(21):2853-61.
19 51. Manzini MC, Tambunan DE, Hill RS, Yu TW, Maynard TM, Heinzen EL, Shianna KV, Stevens
20 CR, Partlow JN, Barry BJ, Rodriguez J, Gupta VA, Al-Qudah AK, Eyaid WM, Friedman JM, Salih MA,
21 Clark R, Moroni I, Mora M, Beggs AH, Gabriel SB, Walsh CA (2012) Exome sequencing and functional
22 validation in zebrafish identify GTDC2 mutations as a cause of Walker-Warburg syndrome. *American*
23 *journal of human genetics.*91(3):541-7.
24 52. Marin-Padilla M (1971) Early prenatal ontogenesis of the cerebral cortex (neocortex) of the
25 cat (*Felis domestica*). I. A Golgi study. I. The primordial neocortical organization. *Z Anat*
26 *Entwicklungsgesch.*134(2):117-45.
27 53. Marin-Padilla M (1998) Cajal-Retzius cells and the development of the neocortex. *Trends in*
28 *neurosciences.*21(2):64-71.
29 54. Martinez-Cerdeno V, Noctor SC (2014) Cajal, Retzius, and Cajal-Retzius cells. *Frontiers in*
30 *neuroanatomy.*8:48.
31 55. Meyer G, Cabrera Socorro A, Perez Garcia CG, Martinez Millan L, Walker N, Caput D (2004)
32 Developmental roles of p73 in Cajal-Retzius cells and cortical patterning. *The Journal of neuroscience*
33 *: the official journal of the Society for Neuroscience.*24(44):9878-87.
34 56. Michele DE, Barresi R, Kanagawa M, Saito F, Cohn RD, Satz JS, Dollar J, Nishino I, Kelley RI,
35 Somer H, Straub V, Mathews KD, Moore SA, Campbell KP (2002) Post-translational disruption of
36 dystroglycan-ligand interactions in congenital muscular dystrophies. *Nature.*418(6896):417-22.
37 57. Moore CJ, Winder SJ (2010) Dystroglycan versatility in cell adhesion: a tale of multiple
38 motifs. *Cell communication and signaling : CCS.*8:3.
39 58. Moore SA, Saito F, Chen J, Michele DE, Henry MD, Messing A, Cohn RD, Ross-Barta SE,
40 Westra S, Williamson RA, Hoshi T, Campbell KP (2002) Deletion of brain dystroglycan recapitulates
41 aspects of congenital muscular dystrophy. *Nature.*418(6896):422-5.
42 59. Muntoni F (2004) Journey into muscular dystrophies caused by abnormal glycosylation. *Acta*
43 *myologica : myopathies and cardiomyopathies : official journal of the Mediterranean Society of*
44 *Myology / edited by the Gaetano Conte Academy for the study of striated muscle diseases.*23(2):79-
45 84.
46 60. Myshrall TD, Moore SA, Ostendorf AP, Satz JS, Kowalczyk T, Nguyen H, Daza RA, Lau C,
47 Campbell KP, Hevner RF (2012) Dystroglycan on Radial Glia End Feet Is Required for Pial Basement
48 Membrane Integrity and Columnar Organization of the Developing Cerebral Cortex. *J Neuropathol*
49 *Exp Neurol.*
50 61. Noctor SC, Flint AC, Weissman TA, Dammerman RS, Kriegstein AR (2001) Neurons derived
51 from radial glial cells establish radial units in neocortex. *Nature.*409(6821):714-20.
52
53
54
55
56
57
58
59
60

- 1
2
3 62. Noctor SC, Palmer SL, Hasling T, Juliano SL (1999) Interference with the development of early
4 generated neocortex results in disruption of radial glia and abnormal formation of neocortical layers.
5 *Cerebral cortex*.9(2):121-36.
- 6 63. Pilz DT, Matsumoto N, Minnerath S, Mills P, Gleeson JG, Allen KM, Walsh CA, Barkovich AJ,
7 Dobyns WB, Ledbetter DH, Ross ME (1998) LIS1 and XLIS (DCX) mutations cause most classical
8 lissencephaly, but different patterns of malformation. *Hum Mol Genet*.7(13):2029-37.
- 9 64. Rakic P (1972) Mode of cell migration to the superficial layers of fetal monkey neocortex. *J*
10 *Comp Neurol*.145(1):61-83.
- 11 65. Roper SN, Abraham LA, Streit WJ (1997) Exposure to in utero irradiation produces disruption
12 of radial glia in rats. *Developmental neuroscience*.19(6):521-8.
- 13 66. Roscioli T, Kamsteeg EJ, Buysse K, Maystadt I, van Reeuwijk J, van den Elzen C, van
14 Beusekom E, Riemersma M, Pfundt R, Vissers LE, Schraders M, Altunoglu U, Buckley MF, Brunner HG,
15 Grisart B, Zhou H, Veltman JA, Gilissen C, Mancini GM, Delree P, Willemsen MA, Ramadza DP,
16 Chitayat D, Bennett C, Sheridan E, Peeters EA, Tan-Sindhunata GM, de Die-Smulders CE, Devriendt K,
17 Kayserili H, El-Hashash OA, Stemple DL, Lefeber DJ, Lin YY, van Bokhoven H (2012) Mutations in ISPD
18 cause Walker-Warburg syndrome and defective glycosylation of alpha-dystroglycan. *Nature genetics*.
19 67. Saillour Y, Carion N, Quelin C, Leger PL, Boddaert N, Elie C, Toutain A, Mercier S, Barthez MA,
20 Milh M, Joriot S, des Portes V, Philip N, Broglin D, Roubertie A, Pitelet G, Moutard ML, Pinard JM,
21 Cances C, Kaminska A, Chelly J, Beldjord C, Bahi-Buisson N (2009) LIS1-related isolated lissencephaly:
22 spectrum of mutations and relationships with malformation severity. *Archives of*
23 *neurology*.66(8):1007-15.
- 24 68. Sarnat HB, Flores-Sarnat L (2003) Etiological classification of CNS malformations: integration
25 of molecular genetic and morphological criteria. *Epileptic disorders : international epilepsy journal*
26 *with videotape*.5 Suppl 2:S35-43.
- 27 69. Sato S, Omori Y, Katoh K, Kondo M, Kanagawa M, Miyata K, Funabiki K, Koyasu T, Kajimura N,
28 Miyoshi T, Sawai H, Kobayashi K, Tani A, Toda T, Usukura J, Tano Y, Fujikado T, Furukawa T (2008)
29 Pikachurin, a dystroglycan ligand, is essential for photoreceptor ribbon synapse formation. *Nat*
30 *Neurosci*.11(8):923-31.
- 31 70. Satz JS, Ostendorf AP, Hou S, Turner A, Kusano H, Lee JC, Turk R, Nguyen H, Ross-Barta SE,
32 Westra S, Hoshi T, Moore SA, Campbell KP (2010) Distinct Functions of Glial and Neuronal
33 Dystroglycan in the Developing and Adult Mouse Brain. *The Journal of Neuroscience*.30(43):14560 –
34 72.
- 35 71. Shinozaki K, Miyagi T, Yoshida M, Miyata T, Ogawa M, Aizawa S, Suda Y (2002) Absence of
36 Cajal-Retzius cells and subplate neurons associated with defects of tangential cell migration from
37 ganglionic eminence in *Emx1/2* double mutant cerebral cortex. *Development*.129(14):3479-92.
- 38 72. Solecki DJ (2012) Sticky situations: recent advances in control of cell adhesion during
39 neuronal migration. *Curr Opin Neurobiol*.22(5):791-8.
- 40 73. Stevens E, Carss KJ, Cirak S, Foley AR, Torelli S, Willer T, Tambunan DE, Yau S, Brodd L, Sewry
41 CA, Feng L, Haliloglu G, Orhan D, Dobyns WB, Enns GM, Manning M, Krause A, Salih MA, Walsh CA,
42 Hurler M, Campbell KP, Manzini MC, Consortium UK, Stemple D, Lin YY, Muntoni F (2013) Mutations
43 in *B3GALNT2* cause congenital muscular dystrophy and hypoglycosylation of alpha-dystroglycan. *Am*
44 *J Hum Genet*.92(3):354-65.
- 45 74. Sugita S, Saito F, Tang J, Satz J, Campbell K, Sudhof TC (2001) A stoichiometric complex of
46 neurexins and dystroglycan in brain. *The Journal of cell biology*.154(2):435-45.
- 47 75. Supèr H, Del Río JA, Martínez A, Pérez-Sust P, Soriano E (2000) Disruption of Neuronal
48 Migration and Radial Glia in the Developing Cerebral Cortex Following Ablation of the Cajal-Retzius
49 Cells. *Cerebral cortex*.10:602-13.
- 50 76. Super H, Martinez A, Soriano E (1997) Degeneration of Cajal-Retzius cells in the developing
51 cerebral cortex of the mouse after ablation of meningeal cells by 6-hydroxydopamine. *Brain Res Dev*
52 *Brain Res*.98(1):15-20.
- 53
54
55
56
57
58
59
60

- 1
2
3 77. Tamamaki N, Nakamura K, Okamoto K, Kaneko T (2001) Radial glia is a progenitor of
4 neocortical neurons in the developing cerebral cortex. *Neuroscience research*.41(1):51-60.
- 5 78. Toda T, Yoshioka M, Nakahori Y, Kanazawa I, Nakamura Y, Nakagome Y (1995) Genetic
6 identity of Fukuyama-type congenital muscular dystrophy and Walker-Warburg syndrome. *Annals of*
7 *neurology*.37(1):99-101.
- 8 79. van Reeuwijk J, Grewal PK, Salih MA, Beltran-Valero de Bernabe D, McLaughlan JM,
9 Michielse CB, Herrmann R, Hewitt JE, Steinbrecher A, Seidahmed MZ, Shaheed MM, Abomelha A,
10 Brunner HG, van Bokhoven H, Voit T (2007) Intragenic deletion in the LARGE gene causes Walker-
11 Warburg syndrome. *Human genetics*.121(6):685-90.
- 12 80. van Reeuwijk J, Janssen M, van den Elzen C, Beltran-Valero de Bernabe D, Sabatelli P, Merlini
13 L, Boon M, Scheffer H, Brockington M, Muntoni F, Huynen MA, Verrips A, Walsh CA, Barth PG,
14 Brunner HG, van Bokhoven H (2005) POMT2 mutations cause alpha-dystroglycan hypoglycosylation
15 and Walker-Warburg syndrome. *Journal of medical genetics*.42(12):907-12.
- 16 81. Vuillaumier-Barrot S, Bouchet-Seraphin C, Chelbi M, Devisme L, Quentin S, Gazal S,
17 Laquerriere A, Fallet-Bianco C, Loget P, Odent S, Carles D, Bazin A, Aziza J, Clemenson A, Guimiot F,
18 Bonniere M, Monnot S, Bole-Feysot C, Bernard JP, Loeuillet L, Gonzales M, Socha K, Grandchamp B,
19 Attie-Bitach T, Encha-Razavi F, Seta N (2012) Identification of mutations in TMEM5 and ISPD as a
20 cause of severe cobblestone lissencephaly. *Am J Hum Genet*.91(6):1135-43.
- 21 82. Weiss KH, Johanssen C, Tielsch A, Herz J, Deller T, Frotscher M, Forster E (2003)
22 Malformation of the radial glial scaffold in the dentate gyrus of reeler mice, scrambler mice, and
23 ApoER2/VLDLR-deficient mice. *J Comp Neurol*.460(1):56-65.
- 24 83. Willer T, Lee H, Lommel M, Yoshida-Moriguchi T, de Bernabe DB, Venzke D, Cirak S,
25 Schachter H, Vajsar J, Voit T, Muntoni F, Loder AS, Dobyns WB, Winder TL, Strahl S, Mathews KD,
26 Nelson SF, Moore SA, Campbell KP (2012) ISPD loss-of-function mutations disrupt dystroglycan O-
27 mannosylation and cause Walker-Warburg syndrome. *Nature genetics*.
- 28 84. Yang AC, Ng BG, Moore SA, Rush J, Waechter CJ, Raymond KM, Willer T, Campbell KP, Freeze
29 HH, Mehta L (2013) Congenital disorder of glycosylation due to DPM1 mutations presenting with
30 dystroglycanopathy-type congenital muscular dystrophy. *Molecular genetics and*
31 *metabolism*.110(3):345-51.
- 32 85. Yang Y, Zhang P, Xiong Y, Li X, Qi Y, Hu H (2007) Ectopia of Meningeal Fibroblasts and
33 Reactive Gliosis in the Cerebral Cortex of the Mouse Model of Muscle-Eye-Brain Disease. *The Journal*
34 *of Comparative Neurology*.505:459-77.
- 35 86. Yeo LY, Matar OK, Perez de Ortiz ES, Hewitt GF (2002) Simulation studies of phase inversion
36 in agitated vessels using a Monte Carlo technique. *J Colloid Interface Sci*.248(2):443-54.
- 37 87. Yoshida-Moriguchi T, Willer T, Anderson ME, Venzke D, Whyte T, Muntoni F, Lee H, Nelson
38 SF, Yu L, Campbell KP (2013) SGK196 is a glycosylation-specific O-mannose kinase required for
39 dystroglycan function. *Science*.341(6148):896-9.
- 40 88. Yoshida A, Kobayashi K, Manya H, Taniguchi K, Kano H, Mizuno M, Inazu T, Mitsuhashi H,
41 Takahashi S, Takeuchi M, Herrmann R, Straub V, Talim B, Voit T, Topaloglu H, Toda T, Endo T (2001)
42 Muscular dystrophy and neuronal migration disorder caused by mutations in a glycosyltransferase,
43 POMGnT1. *Developmental cell*.1(5):717-24.
- 44
45
46
47
48
49
50
51
52
53
54
55
56
57
58
59
60

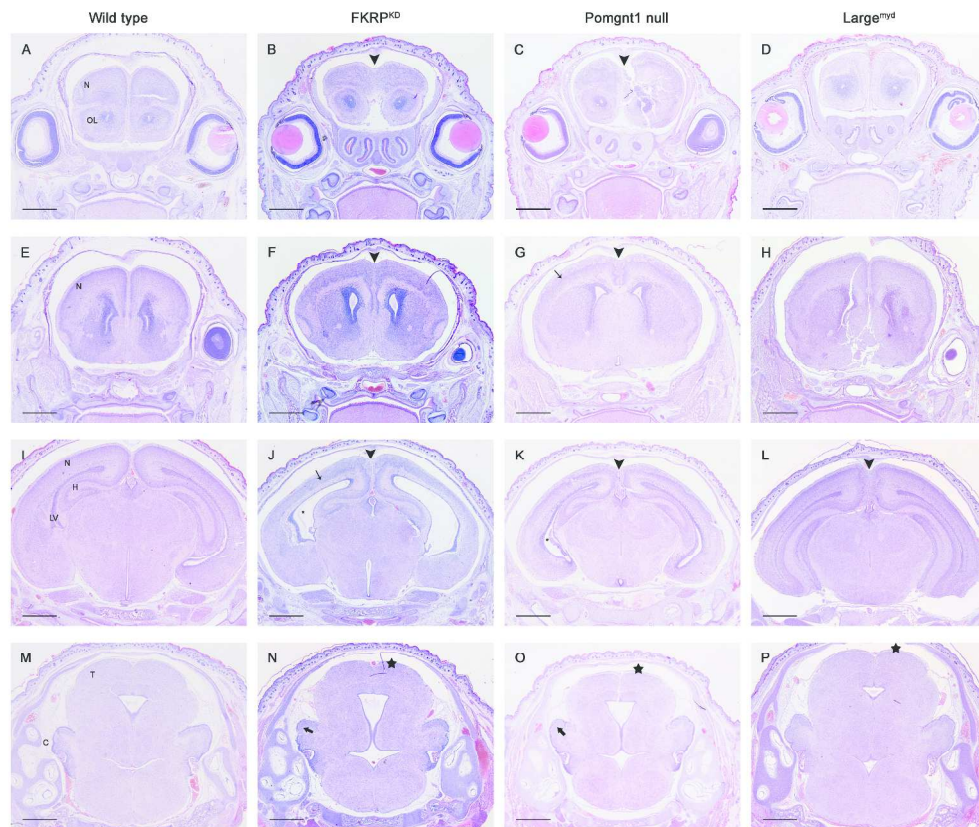


Figure 1: There are substantial histopathological differences in the brain phenotype in FKRPK^{CD}, Pomgnt1^{null} and Large^{myd} mice at P0

A, B, C, D. Olfactory lobes and rostral cortex. In the wild type (A), the organised neocortex is apparent dorsal to the olfactory lobes. In the FKRPK^{CD} and Pomgnt1^{null} mice (B and C, respectively) the olfactory lobes (OL) are normal, but there is interdigitation of the cortical hemispheres (arrow head) and substantial dyslamination of the rostral neocortex. Cortical disorganisation is most apparent in the FKRPK^{CD}. In the Large^{myd} (D), the olfactory lobes are again normal. In these mice the cortical hemispheres remain distinct at this level, but do exhibit disruption in lamination.

E, F, G, H. Cortex around the level of the corpus callosum. The cortical plate is distinct, and overlain by the cell-poor marginal zone in wild type mice (E). In the FKRPK^{CD} (F), the cortex is completely disorganised, and the cortical plate is indistinct. The Pomgnt1^{null} and Large^{myd} mice (G and H, respectively) have well defined cortical plates, but these are overlain by a cell-dense, subarachnoid, extracortical layer, which is more pronounced in the Pomgnt1^{null} mice. In Pomgnt1^{null} mice, the lateral cortex is more disorganised than the medial cortex (fine arrow).

I, J, K, L. Cortex around the level of the hippocampus. At this level, the FKRPK^{CD}, POMGnT1^{null} and Large^{myd} mice (J, K and L, respectively) all exhibit interdigitation of neurons from opposing cortical plates. In the FKRPK^{CD}, the remnants of the cortical plate are apparent medially, with dyslamination increasing laterally (J, fine arrow). There is ventricular dilation in the FKRPK^{CD} and, to a lesser extent the POMGnT1^{null} (*). In addition, there is some rarefaction of the subventricular zone in the FKRPK^{CD} only.

M, N, O, P. Tectum and cerebellum. There is disorganisation of the inferior colliculus, most marked in the FKRPK^{CD} (star). There is some disruption to the granule cell layer of the cerebellum in the FKRPK^{CD} and POMGnT1^{null} (N and O, respectively; bold arrow), when compared to the wild type (M). The cerebellum in the Large^{myd} (P) does not appear to be affected at this time point.

HE. Bars represent 400µm. N = neocortex; OL = olfactory lobes; H = hippocampus; LV = lateral ventricles; T = tectum; C = cerebellum.

1
2
3
4
5
6
7
8
9
10
11
12
13
14
15
16
17
18
19
20
21
22
23
24
25
26
27
28
29
30
31
32
33
34
35
36
37
38
39
40
41
42
43
44
45
46
47
48
49
50
51
52
53
54
55
56
57
58
59
60

466x410mm (300 x 300 DPI)

For Peer Review Only

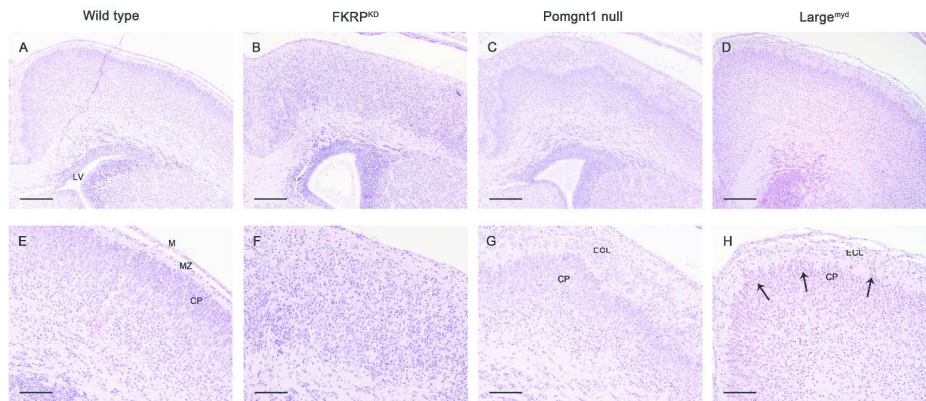


Figure 2: Neocortex at the level corpus callosum.

Neocortex at the level of the corpus callosum. There is consistent fusion of the cortical hemispheres in the FKRP^{KD} (B, F) and the Pomgnt1^{null} (C, G), with interdigitation of neurons from opposing cortical plates. This is not consistently observed in the Large^{myd} at this level (D, H). The degree of disorganisation of the cortical plate varies between models. The cortical plate is inapparent in FKRP^{KD} mice, and no marginal zone is observed. In Pomgnt1^{null} mice the marginal zone and cortical plate are apparent beneath a substantial extracortical layer. The Large^{myd} mice demonstrate a relatively organised cortical plate, but multifocally neurons from the cortical plate are apparent migrating through the marginal zone and the pial basement membrane and running subjacent and tangential to the arachnoid to form a narrow extra cortical layer (fine arrows). The tramline appearance of the normal meninges is not present in FKRP^{KD}, Pomgnt1^{null} and is only multifocally observed in Large^{myd} mice.

HE. A-D – bars represent 400µm; E-F – bars represent 200µm. LV = lateral ventricles; M = leptomeninges; MZ = marginal zone; CP = cortical plate; ECL = extra cortical layer.

490x220mm (300 x 300 DPI)

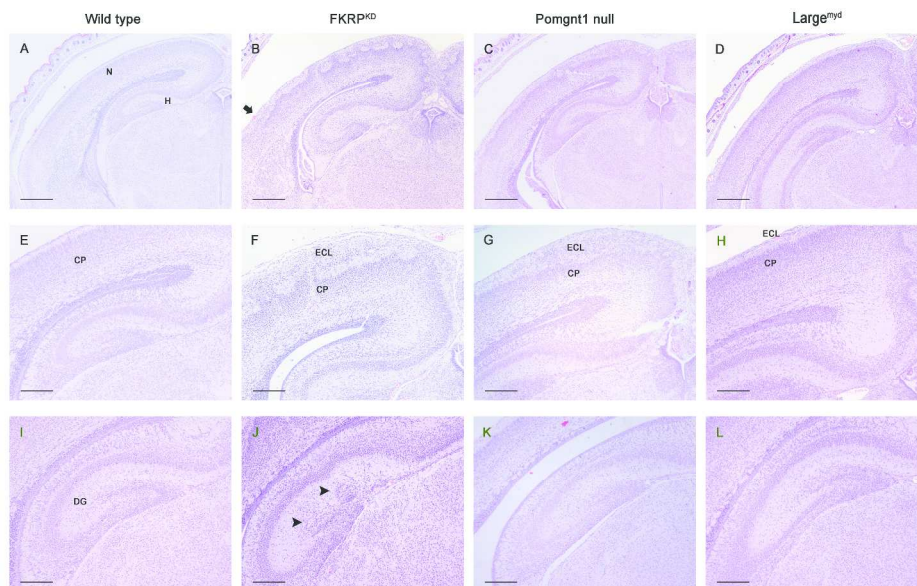


Figure 3: Neocortex at the level of the hippocampus.

For comparison wild type mice are shown in A, E and I. In the neocortex at the level of the hippocampus, laminar architecture is most disrupted in FKRP^{KD} mice, (B, F, J) and to a lesser extent, Pomgnt1^{null} mice (C, G, K). The Large^{myd} mice are least affected (D, H, L). Although the cortex is more organised at this level than rostrally in FKRP^{KD} mice, there is a distinct lateromedial gradient in severity of lesions (bold arrow). There is interdigitation of opposing cortical plates in all mice, including the Large^{myd} at this level. Disruption to the hippocampus, particularly the dentate gyrus, was present in a proportion of the FKRP^{KD} mice (arrowheads), but was not observed in either the Pomgnt1^{null} or the Large^{myd}.

HE. A-D - bars represent 400µm; E-H - bars represent 200µm; I-L - bars represent 100µm. N = neocortex; H = hippocampus; DG = dentate gyrus; ECL = extracortical layer; CP = cortical plate.

495x345mm (300 x 300 DPI)

Only

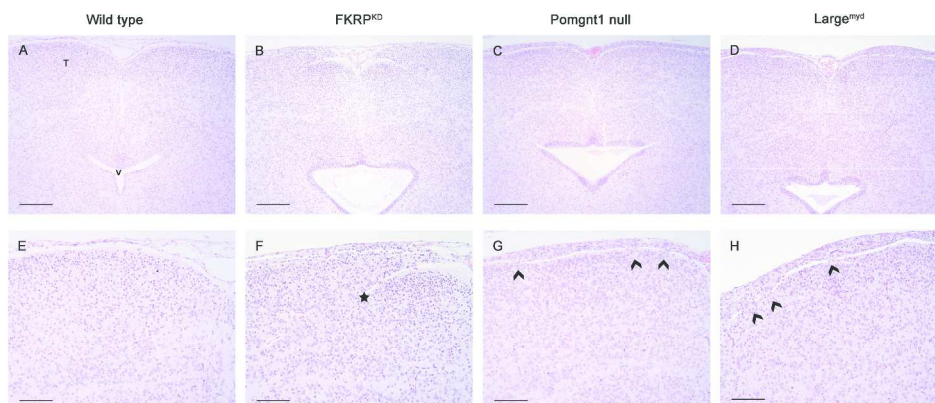


Figure 4: Midbrain at the level of the inferior colliculus

Midbrain: Disorganisation is apparent in the superior and inferior colliculi. For comparison wild type mice are shown in A and E. At this level, the phenotype is similar in the *Pomgnt1*^{null} (C, G) and *Large*^{myd} mice (D, H), with multifocal defects in the pial basement membrane allowing migration of neuron and glial cells into the subarachnoid space (chevrons). In the *FKRP*^{KD} (B, F) there are appear to be more substantial defects in the pial basement membrane laterally (star), allowing a substantial layer of neurons to form above the colliculus itself.

HE. M-P – bars represent 200µm; m-p – bars represent 100µm. T = tectum; V = ventricle.

485x215mm (300 x 300 DPI)

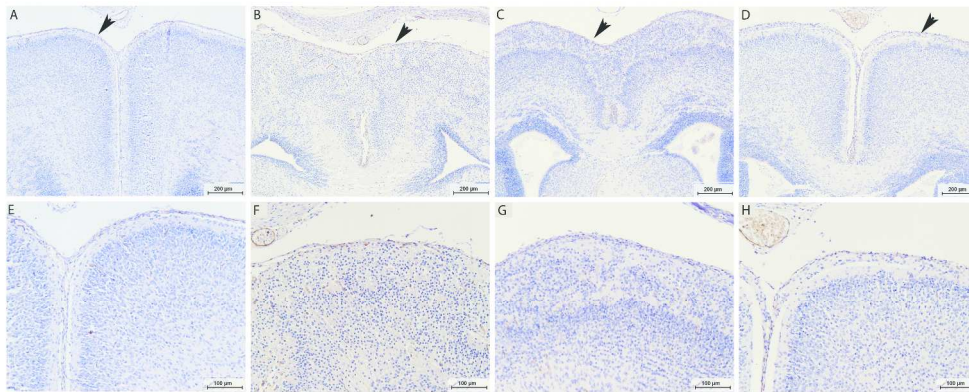


Figure 5B: Immunohistochemical staining for pan laminin to show the glia limitans. A-D. Pan laminin staining of the cortex at the level of the corpus callosum highlighting the location of the glia limitans (see arrow) in the wild type (A), FKR^{KD} (B), Pomgnt1^{null} (C) and Large^{myd} (D). Higher power images are shown in E-H. A-D – bar represents 200μm; E-H – bar represents 100μm.

461x189mm (300 x 300 DPI)

Review Only

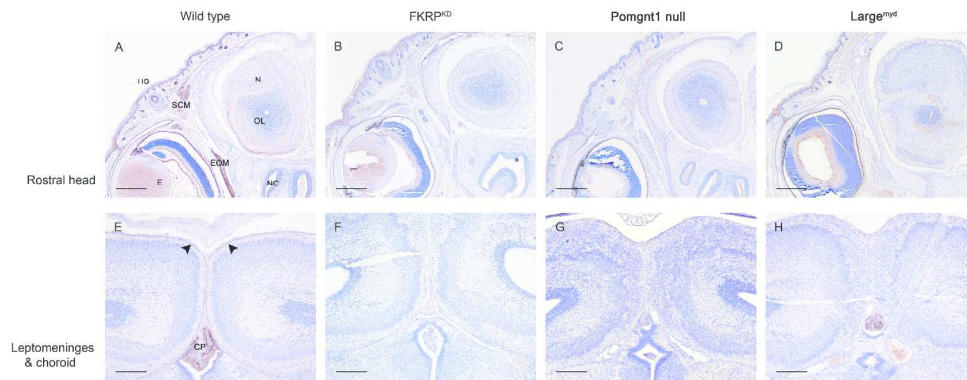


Figure 6. Immunohistochemical staining for the IIH6 epitope of glycosylated alpha dystroglycan in mouse models of dystroglycanopathy

A, B, C, D. Lateral head sections stained with IIH6 antibody. The skin, pial basement membrane and inner limiting membrane of the eye exhibit strong staining in the wild type, in addition to sarcolemmal staining present in the extraocular and subcutaneous muscles (A). Staining of all of these structures is absent in $FKRP^{KD}$ and $Pomgnt1_{null}$ mice (B, C). In $Large^{myd}$ mice (D), the skin remains immunopositive, but staining is absent in other tissues. Bars represent $400\mu m$.

E, F, G, H. IIH6 staining in the brain at the level of the hippocampus. In the WT (E), the basement membrane of choroid plexus is strongly immunopositive and there is a narrow, laminar staining pattern at the pial basement membrane (arrowheads). In the $FKRP^{KD}$ and $Pomgnt1_{null}$ mice (F and G, respectively), no staining is apparent. In the $Large^{myd}$, the basement membrane of the choroid plexus is strongly immunopositive, but there is no staining at the pial basement membrane. Bars represent $200\mu m$. HS = haired skin; SCM = subcutaneous muscle; EOM = extraocular muscle; E = eye; N = neocortex; OL = olfactory lobe; NC = nasal cavity; CP = choroid plexus.

523x218mm (300 x 300 DPI)

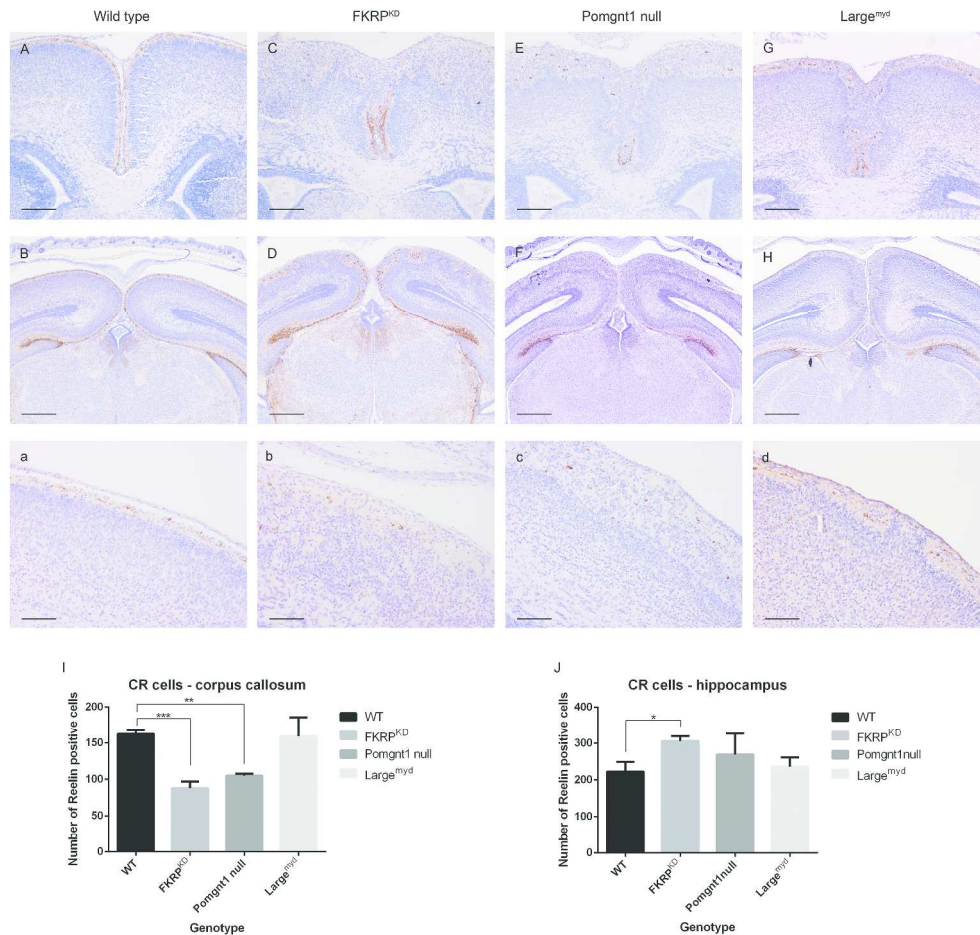


Figure 7: Mislocalisation of the CR cells

Immunohistochemical staining of the Cajal-Retzius cells with an antibody to reelin, at the level of the corpus callosum (A, C, E, G - bar represents 200 μ m) and at the hippocampus (B, D, F, H - bar represents 400 μ m). In wild type mice there are multifocal, tangentially-orientated, reelin-positive Cajal-Retzius cells which form an intermittent, single-cell layer within the marginal zone (A, B). Large numbers of CR cells are present at the hippocampus. In FKRP^{K/D} mice, there is a significant decrease in the number of reelin-positive cells at the level of the corpus callosum (C). Those present are disorganised, haphazardly orientated and predominantly clustered around the anterior cerebral artery. At the level of the hippocampus, more normally distributed and orientated CR cells appear to be associated with more ordered areas of the cortical plate (D). In the POMGNT1^{null} mice (E) there is less clustering of the CR cells around the anterior cerebral artery. CR cells extend further laterally, although are randomly distributed within the extracortical layer. Again, CR cell distribution appears more normal at the level of the hippocampus (F). In the Large^{myd} (G) CR cells are orientated predominantly transversely (as in the wild type) but are overlain by a narrow extracortical layer, rostrally. There is some disruption in the midline at the level of the hippocampus, in areas of fusion of opposing cortical plates (H). a-d. Higher magnification views of the cortex at the level of the corpus callosum, lateral to the interhemispheric fissure (bars represent 100 μ m).

At the level of the corpus callosum (I) there is a statistically-significant decrease in the number of CR cells in FKRP^{K/D} ($P = 0.0002$) and Pomgnt1^{null} mice ($P = 0.0017$), relative to wild type mice (one way ANOVA with Dunnett's multiple comparisons). This is not observed in Large^{myd} mice ($P = 0.986$). At the level of the hippocampus (J) in FKRP^{K/D} there is a statistically-significant increase in the number of CR cells relative to wild type ($P = 0.046$) but no statistically-significant differences in the number of CR cells in either Pomgnt1^{null} or Large^{myd} mice relative to wild type ($P = 0.304$ and $P = 0.930$, respectively).